Optics Letters

47 W continuous-wave 1726 nm thulium fiber laser core-pumped by an erbium fiber laser

Mark D. Burns,* Peter C. Shardlow, Pranabesh Barua, Thomas L. Jefferson-Brain, Jayanta K. Sahu, and W. Andrew Clarkson

Optoelectronics Research Centre, University of Southampton, University Rd., Southampton SO17 1BJ, UK
**Corresponding author: markburns@soton.ac.uk*

Received 24 July 2019; revised 5 September 2019; accepted 9 September 2019; posted 10 September 2019 (Doc. ID 373486); published 21 October 2019

The high-power, short-wavelength operation of a thulium-doped silica fiber laser at 1726 nm has been demonstrated in a core-pumped monolithic (all-fiber) resonator configuration, in-band pumped by a high-power erbium-only fiber laser operating at 1580 nm. The thulium fiber laser yielded 47 W in a single-spatial-mode output beam for 60-W absorbed pump power. The corresponding slope efficiency, with respect to an absorbed pump power of 80%, compares favorably with the theoretical maximum (Stokes) efficiency of 91.5%. The prospects for further scaling of single-mode power in this wavelength regime to >100 W are considered, as well as the potential applications for high-power lasers operating in this difficult-to-reach wavelength band.

https://doi.org/10.1364/OL.44.005230

The wavelength band 1650–1750 nm is of interest due to a variety of spectroscopic features. Of particular significance is the C-H bond stretch resonance overtone between 1610 nm and 1790 nm, which means polymers and other hydrocarbon-containing materials are strongly absorbing within this wavelength band [1–3]. High-power laser sources operating in this spectral region could be utilized for the efficient processing of transparent plastics, avoiding the need for additives to increase the absorption when employing traditional 1 μm ytterbium (Yb) doped laser sources. Thulium (Tm) doped fiber lasers with operating wavelengths >2 μm are already utilized in the processing of a range of plastics [4], but there are significant benefits to be gained by operating at shorter wavelengths in terms of enhanced absorption. For example, Polyethylene has an absorption coefficient approaching ~11.5 $dBmm^{-1}$ at ~1.7 μm, but only ~1.2 $dBmm^{-1}$ at ~2.1 μm [4]. In addition to potential applications in laser polymer processing and the processing of other hydrocarbon-containing materials, laser sources in the 1650–1750 nm region have several other promising applications such as environmental sensing, and various medical applications due to a local water absorption minimum at 1720 nm [3,5].

Laser sources boasting high average output power in the 1 μm band, based on Yb-doped fiber or disk geometries, have become commonplace. Tm-doped fiber lasers operating in the 1.9–2.1 μm region have emerged as contenders, steadily advancing in terms of average output power and deployment in a growing number of applications. However, operating lasers at high power in the 1650–1750 nm band has proved much more challenging. This region lies between the wavelength bands where Erbium (Er) doped and Tm-doped lasers traditionally work well. The emission band for Tm-doped silica is very broad, extending from ~1650 nm to >2100 nm [6,7], and hence covers the wavelengths of interest. However, the strong quasi-three-level character and the associated reabsorption loss makes it extremely difficult to achieve a population inversion and net gain utilizing conventional cladding-pumping with 790 nm diode pump sources. Thus, power scaling has generally been restricted to the longer wavelength end of the Tm emission spectrum. Accessing the short-wavelength region mandates the use of a higher-brightness pump source in conjunction with a core-pumped (or small inner-cladding-to-core area ratio) configuration. In the past, this has been achieved by direct (in-band) pumping using cladding-pumped erbium/ytterbium (Er/Yb) co-doped fiber lasers [8]. This approach has the attraction of a low quantum defect (<10%) in the Tm laser at 1.7 μm, and low Tm concentrations can be used to further distribute pump absorption and heat loading (as required). Er-doped fibers are commonly co-doped with Yb to significantly increase pump absorption efficiency while allowing the erbium ion concentration to be kept low to limit pair induced quenching (PIQ) [9]. However, power scaling of single-mode Er/Yb fiber lasers is limited due to the onset of parasitic lasing or amplified spontaneous emission (ASE) on the Yb transition. This unwanted emission around 1 μm reduces device efficiency at high pump powers, and, due to the onset of self-pulsing, can cause catastrophic damage to the fiber and pump diodes. This issue has greatly restricted powers from single-mode Er/Yb fiber sources, and, as a result,

power scaling of short-wavelength Tm fiber lasers has so far been limited to 12.7 W via this route [8]. Bismuth-doped germanosilicate fiber offers wavelength coverage of around 1.6 μm to 1.8 μm, potentially ideal for accessing the target spectral band. However, to date, the highest CW output power in the region of 1.7 μm using these fibers is 1 W, pumped at 1.6 μm. The slope efficiency of 33% was limited by the propagation losses incurred due to long device lengths [10]. Raman fiber lasers also offer a route to hard-to-reach spectral bands. In particular, 1 μm pumped random Raman fiber lasers have expressed high powers up to the ninth Stokes, including 70 W at 1676 nm [11], limited by the onset of higher-order Stokes components but with scope for further scaling. Raman fiber lasers pumped at 1.6 μm are more directly able to access the 1.7 μm region but are so far limited to 6 W for single-mode sources [12].

Here, we report an alternative strategy for power scaling short-wavelength Tm fiber lasers, employing an Er-only fiber laser pump source, that yielded 47 W of single-mode output at 1726 nm. Er-only-doped fiber lasers offer the prospect of power scalability without the detrimental impact of parasitic lasing at 1 μm, but they are nevertheless challenging to scale in output power in cladding-pumped laser configurations, owing to the need for relatively low Er doping levels to avoid significant PIQ. The target Er ion concentration of 1×10^{25} m^{-3} was chosen following the design rationale reported by Kotov *et al.* [13], who found that this doping level is optimal for Er-only fiber lasers, giving the best compromise between pump absorption efficiency, PIQ, and device performance when operating in the 1580–1590 nm band. Our preform was fabricated via modified chemical vapor deposition (MCVD) and solution doping, with three layers of Er-doped aluminosilicate, to yield a relatively large core section with a numerical aperture (NA) of 0.08. The surrounding pure silica inner cladding was machined with a CO_2 laser to produce an octagonal cross-sectional shape, as required for improving the pump absorption efficiency [14]. Given the restrictions on the Er doping level, key design parameters are the core diameter and core-to-cladding area ratio. These parameters must be carefully optimized to minimize the required fiber length for efficient pump absorption, reducing unwanted background loss, while at the same time, maintaining robust single-mode operation. This resulted in a final Er fiber design with a core diameter of 21 μm (V-number ≈3.3), a mode field diameter (MFD) of 18 μm at 1580 nm, and an inner-cladding (flat-to-flat) size of 122 μm. This dimension was selected to match the area of a circular 125 μm diameter fiber in order to minimize cladding loss at splices between active sections and passive sections of fiber. The Er fiber was coated with a low refractive index ($n = 1.375$) fluorinated polymer coating to yield a high effective NA (>0.4) for the inner-cladding pump guide. The absorption coefficient for pump radiation at 976 nm launched into the inner cladding was measured via the cutback technique to be 0.22 dBm^{-1}. As a result, the fiber device length was selected as 38 m as a compromise between the pump absorption efficiency and the background propagation losses (measured as −40 $dBkm^{-1}$), to yield a −8.4 dB pump absorption efficiency. The use of a large core area necessitated the use of additional bend-induced loss to suppress unwanted higher order modes. This was achieved by coiling the fiber with a 50 mm radius, which produces a calculated additional loss of −600 dBm^{-1} for the $LP_{1,1}$ mode, but less than −0.01 dBm^{-1} extra loss for the fundamental ($LP_{0,1}$) mode.

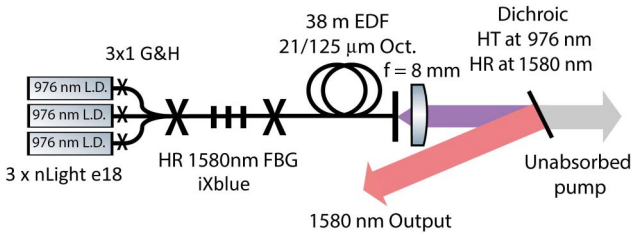

Fig. 1. System schematic for the erbium-doped fiber (EDF) laser. (HR 1580 nm FBG: high reflectivity fiber Bragg grating at 1580 nm.)

The experimental setup for the Er fiber laser is shown in Fig. 1. The cavity was formed between an $R > 99.6\%$ high reflectivity (HR) fiber Bragg grating (FBG), centered at 1580 nm, and the broadband Fresnel reflection of 3.3% from a perpendicular flat cleave, which served as the output coupler (OC). The fiber was spooled onto a water-cooled aluminum cylinder to achieve the desired bend radius and to facilitate thermal management. A pump light was provided by three 135 W diode lasers at 976 nm (nLIGHT), combined via a 3×1 tapered fiber bundle (TFB) (Gooch and Housego) and launched through the HR FBG (IXBlue). The output beam was collimated with the aid of an 8 mm focal length antireflection-coated aspheric lens and separated from the remaining (unabsorbed) pump light using a short-pass dichroic filter.

The output power for the Er fiber laser is plotted as a function of both launched pump power and absorbed pump power in Fig. 2. At the maximum launched power of 400 W (325 W absorbed), the laser yielded an output power of 95 W. The diode pumps were equipped with wavelength control by a volume Bragg grating (VBG), which was effective in stabilizing the operating wavelength at 976 nm only at powers >300 W. The slope efficiency with respect to absorbed pump power was 30%, and once the diodes had locked onto the VBG, the slope efficiency, with respect to the launched pump power, was 24%. No efficiency rolloff is observed in the output power versus the pump power. Moreover, due to the low pump absorption coefficient and hence the distributed thermal load, the outer surface temperature of the fiber (measured with a FLIR thermal

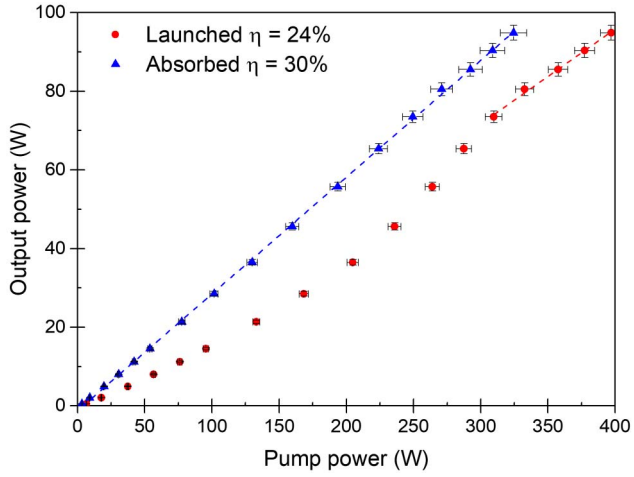

Fig. 2. Output power for the Er fiber laser plotted against both launched pump power and absorbed pump power, yielding slope efficiencies (η) of 24% and 30%, respectively.

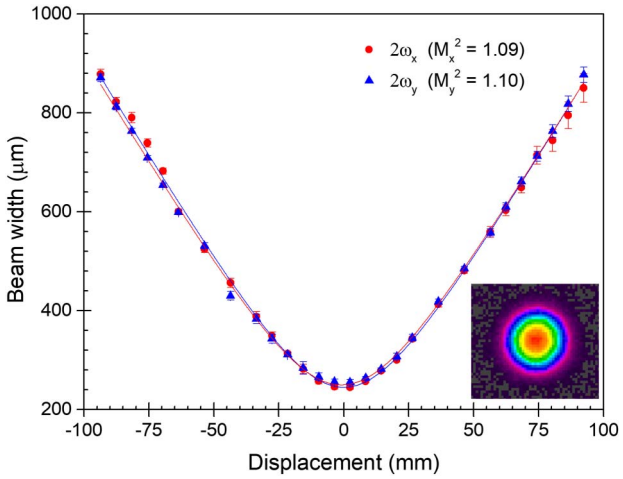

Fig. 3. M^2 measurement of the erbium-doped fiber laser. $M_x^2 = 1.09$ and $M_y^2 = 1.10$. Inset: the beam profile captured using a Spiricon Pyrocam.

camera) did not exceed 40°C at the hottest point. This suggests that further scaling of output power to well over 100 W should be possible with a higher power and a higher brightness diode pump source. The output beam profile, measured with the aid of a pyroelectric camera (Spiricon Pyrocam), shown in the inset of Fig. 3, was confirmed to be purely fundamental mode ($LP_{0,1}$). Using an Ophir Nanoscan beam-profiler, the beam propagation factors (M_x^2 and M_y^2) in orthogonal planes were measured to be 1.09 and 1.10, respectively (see Fig. 3).

The experimental setup for the Tm fiber laser is shown in Fig. 4. The Tm fiber used in this arrangement was fabricated in-house via MCVD and solution doping. The resulting fiber had a single-mode Tm-doped alumina-silicate core with a 10 μm diameter, a calculated MFD of 11 μm, and 0.13 NA (V-number = 2.37) [8]. A relatively low Tm concentration (0.2 wt. %) was used to distribute the thermal load, primarily due to quantum defect heating, and avoid any additional heating due to energy-transfer-upconversion (ETU). The fiber had

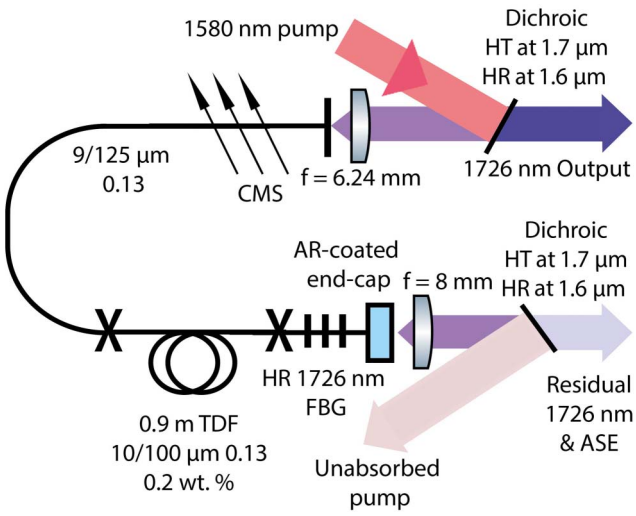

Fig. 4. Schematic of the thulium-doped fiber laser. (HR 1726 nm FBG: high reflectivity fiber Bragg grating at 1726 nm.)

a 100 μm diameter pure silica cladding and, although not intended for use in cladding-pumped configurations, was coated with a low index polymer coating. The latter was chosen in preference to a standard high index coating to reduce the likelihood of damage due to stray laser light coupled into the cladding from imperfect splices between the gain and passive fiber sections. The laser cavity was configured with sections of matched passive fiber spliced to both ends of the Tm fiber. Feedback for lasing was provided by an $R > 99.9\%$ FBG at 1726 nm located in one section of passive fiber and, at the opposite end, by a ∼3.4% Fresnel reflection from a perpendicularly cleaved fiber facet in the other section of passive fiber serving as the OC. Pump light from the Er fiber laser was coupled into the Tm fiber via the output coupler with the aid of an antireflection coated aspheric lens ($f = 6.24$ mm). Pumping through the OC was chosen to minimize the pump power incident on the FBG, a precaution against damage due to scattered pump light. A sufficient length of Tm fiber (∼0.9 m) was used to ensure almost complete absorption (–21 dB) of the launched pump light. The Tm fiber section was coiled, and surface mounted on a water- cooled aluminum plate. A cladding-mode-stripper (CMS) was incorporated into the passive lead-in fiber to remove any stray pump light not coupled into the core as a precaution against damage due to absorption in the fiber coating in any single-clad sections (i.e., the FBG). The CMS was fabricated in-house using a CO_2 laser to machine a series of notches into a stripped section of the passive fiber [15]. The output from the Tm fiber was extracted with the aid of a dichroic mirror with high transmission at 1726 nm and a high reflectivity at 1580 nm. At the opposite end of the fiber (i.e., beyond the FBG), an antireflection-coated bulk fused silica endcap was fused to the fiber end facet to suppress broadband feedback that might otherwise lead to parasitic lasing at longer wavelengths. Residual Tm laser emission transmitted through the FBG, together with ASE and unabsorbed pump light, was monitored using a long-pass dichroic filter to separate pump from ASE and signal light. The output power from the Tm fiber laser is plotted against absorbed pump power in Fig. 5. It should be noted that the slope efficiencies, with respect to the absorbed pump power and the launched power, are comparable due to the high pump absorption efficiency. The laser produced a maximum output power of 47 W at 1726 nm for 60 W of absorbed pump power, corresponding to a slope efficiency of 80%. This compares favorably with the theoretical upper limit on slope efficiency of 91.5%. The difference is attributed to splice losses between the Tm fiber section and the passive fiber section and a small mismatch in core parameters (estimated as –0.08 dB per splice). The inset in Fig. 5 shows the laser spectrum, confirming laser output at 1726 nm with the ASE background at 50 dBm below the laser emission peak. At maximum output power, the combined residual signal and ASE powers were less than 100 mW. The beam propagation factors (M_x^2 and M_y^2) were measured to be 1.05 and 1.01, respectively, thus confirming single-mode operation as also evidenced by the beam profile (see Fig. 6 and inset).

In summary, we have demonstrated 47 W of single-mode output from a Tm fiber laser at 1726 nm, with slope efficiency with respect to absorbed pump power of 80%. Further optimization of the laser design to reduce splice losses, improve the coupling efficiency, and increase the output power of

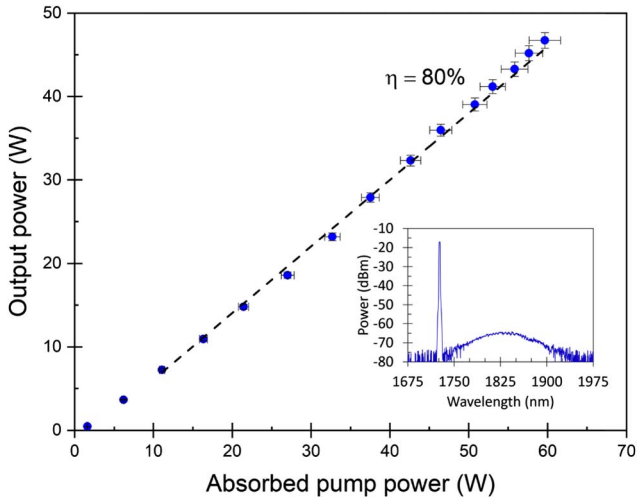

Fig. 5. Output power versus absorbed pump power for the Tm-doped fiber laser with corresponding slope efficiency (η) of 80%. Inset: output spectrum for Tm fiber laser.

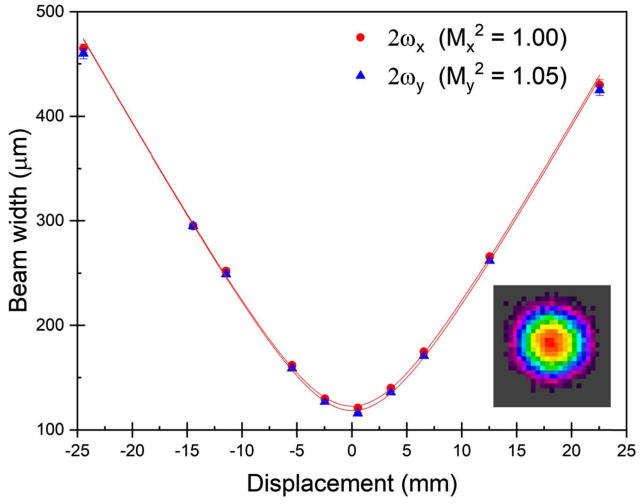

Fig. 6. M^2 measurement of the thulium-doped fiber laser. $M_x^2 = 1.05$ & $M_y^2 = 1.01$. Inset: the beam profile captured using a Spiricon Pyrocam.

the Er pump laser offer the prospect of output powers greater than 70 W. Given the flexibility in the Tm fiber design, including the option to use even lower Tm concentrations to further distribute thermal load and allow straightforward fabrication of large-mode-area designs, it should be possible to scale single-mode powers in this wavelength band into the multi-hundred-watt regime and beyond. The main prerequisite will be a higher-power single-mode Er fiber laser. The 1650–1750 nm band is rich in spectroscopic features and laser sources offering high power, high brightness, and wavelength flexibility in this wavelength regime will benefit a wide range of applications in areas such as medicine and industrial laser processing.

Funding. Engineering and Physical Sciences Research Council (1921150, 1921199).

Acknowledgment. The data underpinning this publication is available from the University of Southampton repository at https://doi.org/10.5258/SOTON/D0939.

REFERENCES

1. K. Jansen, M. Wu, A. van der Steen, and G. van Soest, Photoacoustics **2**, 12 (2014).
2. R. Klein, *Laser Welding of Plastics* (Wiley, 2012), pp. 36–55.
3. F. H. Sakamoto, A. G. Doukas, W. A. Farinelli, Z. Tannous, M. Shinn, S. Benson, G. P. Williams, J. F. Gubeli, H. F. Dylla, and R. R. Anderson, Lasers Surg. Med. **44**, 175 (2012).
4. I. Mingareev, F. Weirauch, A. Olowinsky, L. Shah, P. Kadwani, and M. Richardson, Opt. Laser Technol. **44**, 2095 (2012).
5. S. P. Garaba, J. Aitken, B. Slat, H. M. Dierssen, L. Lebreton, O. Zielinski, and J. Reisser, Environ. Sci. Technol. **52**, 11699 (2018).
6. S. D. Agger and J. H. Povlsen, Opt. Express **14**, 50 (2006).
7. S. D. Jackson and T. A. King, J. Lightwave Technol. **17**, 948 (1999).
8. J. M. O. Daniel, N. Simakov, M. Tokurakawa, M. Ibsen, and W. A. Clarkson, Opt. Express **23**, 18269 (2015).
9. J. E. Townsend, W. L. Barnes, K. P. Jedrzejewski, and S. G. Grubb, Electron. Lett. **27**, 1958 (1991).
10. N. K. Thipparapu, Y. Wang, S. Wang, A. A. Umnikov, P. Barua, and J. K. Sahu, Opt. Mater. Express **9**, 2446 (2019).
11. L. Zhang, J. Dong, and Y. Feng, IEEE J. Sel. Top. Quantum Electron. **24**, 1400106 (2018).
12. R. Thouroude, H. Gilles, B. Cadier, T. Robin, A. Hideur, A. Tyazhev, R. Soulard, P. Camy, J.-L. Doualan, and M. Laroche, Laser Phys. Lett. **16**, 025102 (2019).
13. L. V. Kotov, M. E. Likhachev, M. M. Bubnov, O. I. Medvedkov, M. V. Yashkov, A. N. Guryanov, S. Février, J. Lhermite, and E. Cormier, Proc. SPIE **8961**, 89610X (2014).
14. P. C. Shardlow, R. Standish, J. Sahu, and W. A. Clarkson, "Cladding shaping of optical fiber preforms via CO_2 laser machining," in *European Conference on Lasers and Electro-Optics—European Quantum Electronics Conference*, Munich, Germany (Optical Society of America, 2015).
15. K. Boyd, N. Simakov, A. Hemming, J. Daniel, R. Swain, E. Mies, S. Rees, W. A. Clarkson, and J. Haub, Appl. Opt. **55**, 2915 (2016).